Adsorption of Pyridine on the Gold(111) Surface: Implications for "Alligator Clips" for Molecular Wires

Ante Bilić and Jeffrey R. Reimers*

School of Chemistry, The University of Sydndey, NSW 2006, Australia

Noel S. Hush

School of Chemistry and Department of Biochemistry, The University of Sydney, NSW 2006, Australia

Received: March 1, 2002; In Final Form: April 25, 2002

The adsorption of pyridine on metal surfaces such as gold(111) is an important and much studied process in solution, but little is known about the adsorption of isolated pyridine molecules. We determine the structure, binding energy, and dipole moment for this system using the PW91 density functional, periodic imaging, a plane-wave basis set, and ultrasoft pseudopotentials. Significant binding is found only for atop configurations in which pyridine sits vertically above a single gold atom with its nitrogen bound to the gold. For this configuration, the calculated binding strength, after extrapolation to zero coverage is 8.4 kcal mol^{-1}, a value that is qualitatively realistic but quantitatively may be too small in order to explain known free energies of formation from solution. The binding is insensitive to tilting of the pyridine by up to 30° from vertical, but a sizable energy of order 5 kcal mol^{-1} is predicted to be required in order to drive pyridine flat above the surface. Qualitative arguments based on analysis of the PW91 results combined with approximate estimates of the dispersion energy suggest that the binding is essentially dispersive in nature. While the application of density functional theory to problems of this type is problematic, earlier results obtained using PW91 for the analogous binding of ammonia to gold indicate that the computational method used is appropriate, at least for vertical atop adsorption.

I. Introduction

The interaction of aromatic molecules with metal surfaces has attracted increasing interest because of the need to understand and control monolayer properties. For this, the properties of weak binding such as physisorption and intermolecular interactions are often of central importance. A traditional interest in this problem has long existed in the field of catalysis owing to the importance of metals as catalysts for ring-cracking reactions.[1] This exploits the possibility of the occurrence of much stronger interactions with the surface. In recent years, a new interest in these interface-related processes has arisen in the design of molecular electronic devices in which a single molecule or films are used to span two metal (e.g., gold) electrodes.[2−7] In this environment, the bonding pattern is unique as, in common with the catalysis problem, only single molecule to surface interactions are important while, in common with monolayer formation, only weak interactions are involved. Here, we study the binding of pyridine to gold(111). Pyridine and other azine bases such as 1,10-phenanthroline have been used to secure molecular wires to metal atoms and metal surfaces,[8−10] and their interaction with the gold(111) surface is of particular interest. In principle, quite different binding between a single pyridine molecule and a pyridine incorporated in a monolayer could occur, however, owing to the anticipated relative weakness of the molecule−surface interaction and the possibly competitive strength of inter-pyridine interactions present only in the monolayer. While much is known about pyridine monolayers on gold,[11,12] little is known about its adsorption from vacuum in the low-coverage limit.

The adsorption of pyridine in the ultrahigh vacuum (UHV) has been studied on various single-crystal surfaces of a variety of metals including Pt, Ni, Pd, Ir, Cu, Pt, and Ag. The summary of results, shown in Figure 1 ref 13, indicates that the orientation of pyridine varies as a function of coverage and temperature and is also dependent on the type and structure of the substrate. A significant feature is that pyridine can be bound to a surface either via the delocalized π electrons of its carbon ring or through the electron lone pair of its nitrogen. Hence, depending on the relative contributions of the lone pair and π-ring, the molecule can be tilted with respect to the substrate surface. Its ring can be parallel with it, or it can stand upright, bound solely via the N lone pair. In addition, partial dehydrogenation has also been observed on some substrates (not gold or silver) to form α-pyridyl species bonded through both the nitrogen and the α-carbon of the ring. With the exception of Cu(110), on which pyridine always sticks perpendicularly to the surface,[14] the adsorption on all other substrates exhibits dependence of the orientation on the coverage and temperature.

The adsorption of pyridine on Au(111) has been studied electrochemically (see, e.g., ref 11 and references therein) in solution, but no studies have been performed using UHV conditions. UHV studies have been performed for the analogous problem of the adsorption of pyridine to silver(111), however, using vibrational[15] and electronic[16] spectroscopy, leading to somewhat different conclusions. The vibrational study[15] concluded that at low coverages pyridine sticks to the surface flat, through the π-ring, while at the higher coverage of ∼0.5

* Corresponding author. E-mail: Reimers@chem:usyd.edu.au.

10.1021/jp020590i CCC: $22.00
Published on Web 06/12/2002

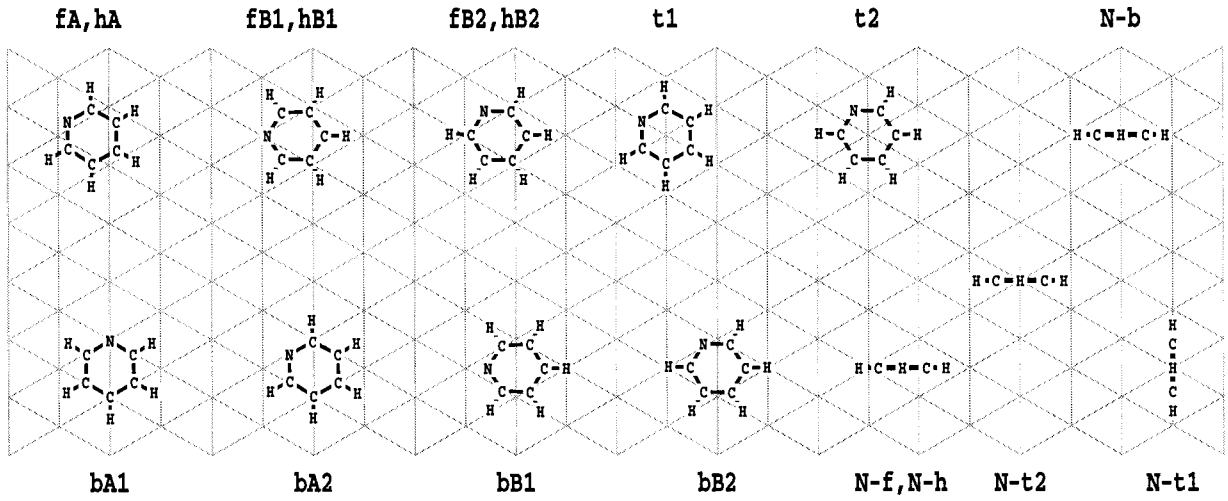

Figure 1. Initial guess for adsorption sites of pyridine on Au(111). Structures bA1, bA2, bB1, and bB2 are flat with the ring-center above bridge sites; fA, hA, fB1, hB2, and hB2 are flat with the ririg-center above either fcc (f) or hcp (h) hollow sites; t1 and t2 are flat structures with the ring-center above a gold atom; and N−b, N−f, N−h, N−t1, and N−t2 are top (vertical) structures with the nitrogen above bridge, fcc hollow, hcp hollow, and top (eclipsed and staggered) sites, respectively.

monolayers (ML) it undergoes a phase transition to a tilted N-bonded phase. Alternatively, the electronic study[16] concluded that at all coverages pyridine adsorbs through the N lone pair, with the tilt angle between the surface and molecule plane varying between 45° and 70°. This difference reflects the difficulty in performing and analyzing experimental measurement of the properties of interest and raises the possibility that the structure of gold(111)−pyridine could be significantly different from that of silver(111)−pyridine. Indeed, pyridine is known to adsorb more strongly to gold than to silver.[12]

An alternate approach to understand the properties of the interface is via computation. This has been done for a closely related system, 4-cyanopyridine (4-CP) on Au(111),[17] at the level of Møller−Plesset perturbation theory (MP2), modeling the substrate by a cluster. The results predict that the most stable configuration is vertical, with 4-CP coordinated to the surface through the N atom of the pyridine ring. A considerable binding energy of 1.45 eV (33.5 kcal mol^{-1}) was obtained, suggesting that pyridine−pyridine interactions would be too weak to exert an influence on the structure at high coverage. In general, the application of the MP2 method to metals is expected to significantly overestimate the binding energy owing to the low-energy denominators involved in the perturbation expansion. We have performed extensive calculations of the properties[18] of $AuNH_3$ and of NH_3 bonded to Au(111) and find that charge transfer between ammonia and gold clusters is important, significantly enhancing the bonding, while analogous charge transfer with the metal surface does not occur. Hence, cluster calculations are also likely to significantly overestimate the binding energy. Last, we have also shown[18] that the very small basis sets used in the MP2 calculations lead to dramatic overestimates of the binding. It is thus clear that an improved computational scheme is required.

Here, results from calculations of the adsorption of pyridine on the Au(111) surface are reported. These employ density functional theory using the PW91 density functional.[19] Previously,[18] we have examined the performance of PW91 in describing the somewhat analogous binding in $AuNH_3$ and find that it produces potential-energy surfaces of excellent shape but underestimates the binding strength after spin−orbit and other corrections by ca. 3 kcal mol^{-1} or 20%. We have also examined[20] in detail the binding of ammonia to gold(111) and found the attraction to be largely dispersive in nature, with PW91 representing this term empirically through an effective covalent interaction. The use of density-functional theory in situations for which the primary attractions are dispersive is problematic,[21] with applications needing to be considered on an individual basis. Nevertheless, the good results that we have obtained for gold−ammonia interactions suggest that this method may also be adequate for the study of gold−pyridine binding; much poorer performance is expected for other commonly used density functionals.[18]

II. Methodology

All computations were performed using the Vienna ab initio simulation package (VASP).[22,23] This utilizes an iterative scheme to solve self-consistently the Kohn−Sham equations of density functional theory using residuum-minimization techniques and an optimized charge-density mixing routine. A plane-wave basis set is employed to expand the electronic wave functions, which facilitates the evaluation of the Hellmann−Feynman forces acting on atoms. Electron−ion interactions are accounted for through the use of pseudopotentials,[24,25] which allows the use a low-energy cutoff for the plane-wave basis set. Their use for nitrogen is known[18] to result in the underestimation of the binding strength of a gold atom to ammonia by 3 kcal mol^{-1} but is required for computational efficiency, as explicit treatment of 1s electrons would require an excessive number of plane-wave basis functions. For electron−electron exchange and correlation interactions the functional of Perdew and Wang[19] (PW91), a form of the generalized gradient approximation (GGA), is used in the current work. It is chosen as, from a variety of density functionals, this is the only one found[18] to provide a realistic description of AuNH3, and it is also known to provide a good description of NH3 bound to gold(111).[20] The irelaxation of atom positions is performed via the action of a conjugate gradient optimization procedure.

The gold surface was modeled by supercells consisting of several atomic layers and vacuum. The application of periodic boundary conditions in all three Cartesian directions yields an infinite array of periodically repeated slabs separated by regions of vacuum. The slab was 4 atomic layers thick while the vacuum was 10; the interlayer spacing is taken from the previously determined[20] value of the bulk lattice parameter, 4.2 Å. One pyridine molecule was placed in the vacuum region on each

TABLE 1: Adsorption Energies (kcal mol^{-1}) for Pyridine in Various Conformations on the Au(111) Surface at 1/9 ML Coverage[a]

N-t1	N−t2	N−b	N−f	N−h	t1	t2	bA1	bA2	bB1	bB2	fA	fB1	fB2	hA	hB1	hB2
7.3	7.2	2.5	1.9	1.8	2.0	1.9	2.0	2.0	2.3	2.0	2.1	2.3	2.1	2.1	2.4	2.1

side of the slab with an approximate inversion center; this configuration is chosen in order to reduce long-range intercell dipole−dipole interactions. For most calculations, a (3 × 3) superstructure was used for the layers resulting in nine gold atoms per layer. This represents a 1/9 ML coverage, sufficiently low that the pyridine molecules in neighboring cells are well separated. To gain insight into the effects of adsorbate−adsorbate interactions on the energetics and geometry a few computations for vertically oriented pyridine were also performed for a 1/4 ML coverage corresponding to a (2 × 2) lateral geometry. This facilitates the extrapolation of the binding energies to the zero coverage limit. In all calculations, the top and bottom layers were allowed to relax, with inner layers frozen in the bulk positions. Our slab thickness of just 4 layers is too small to produce converged binding energies that are insensitive to the relative positioning of the pyridine molecules on each side of the slab. For the binding of NH3 to gold(111) we investigated the analogous problem thoroughly[20] and found for the strongly bound vertical alignment of the adsorbate that calculations of the type we perform herein are likely to be in error by at most 1 kcal mol^{-1} due to this effect.

Brillouin-zone integrations have been done using a 5 × 5 × 1 **k**-point Monkhorst-Pack grid with a Methfessel−Paxton smearing[26] of 0.2 eV. An energy of 350 eV, dictated by the pseudopotential of nitrogen, has been set as the cutoff in all computations involving surfaces or pyridine. Expansion of this cutoff indicates that the results obtained are in the complete-basis-set limit.

III. Results

A. Uncomplexed Pyridine. The energy and geometry of pyridine in the gas phase have been evaluated using two molecules with an inversion center in a cell of the same size as the (3 × 3) supercell. The optimized bond lengths and angles are provided in Supporting Information and are in excellent agreement with the experimental[27] and high-level computational[28] values. As polarization[20] and charge-transfer[18] effects are important in gold to nitrogen lone-pair binding, it is important that the computational method provides realistic estimates for the dipole moment and ionization energies of the free adsorbate, respectively. The calculated dipole moment is 2.25 D and is in good agreement with the observed value of 2.215 D.[27] Also, the Kohn−Sham eigenvalues provide estimates of the vertical ionization energies of the adsorbate. These are provided in Supporting Information along with experimental values[29] for the lowest 12 valence ionizations; they are consistent with previous calculated values.[30] The correct ordering is predicted except for one pair, but the eigenvalues consistently underestimate the ionization energies by ca. 4 eV. Explicit evaluation of the PW91 ionization energies through evaluation of the energy of the molecular cations reduces this discrepancy by an order of magnitude, indicating that the deviation arises from the failure inherent in all known density functionals to reproduce the correct asymptotic potential. It is a feature that restricts the applicability of modern density functionals for problems involving charge transfer, and its significance to pyridine-gold binding is discussed later.

B. Adsorbate Structure. Geometries of the adsorbate have been fully optimized upon placing the molecules in a high-symmetry orientation in the vicinity of the (3 × 3) slab, with either the center of the ring or the nitrogen atom above a binding site. Pyridine adsorption has been considered on top, bridge, and two 3-fold hollow sites (fcc and hcp) for twelve flat and four vertical configurations, as indicated in Figure 1. In addition, for each of the four vertical configurations azimuthal scans around the molecule C_{2v} axis for the favorable orientation have been carried out, with results for two key atop arrangements N−t1 and N−t2 shown explicitly in the figure. The adsorption energies for the optimized structures are listed in Table 1. Apart from the atop adsorption, for which adsorption energies of 7.3 and 7.2 kcal mol^{-1} for N−t1 and N−t2, respectively, have been evaluated, all sites show rather weak binding with adsorption energies varying between 1.8 and 2.5 kcal mol^{-1}.

It is apparent from Figure 1 that the atop structure N−t1 and the flat structures hB1 and fB1 are related by a simple rotation of the pyridyl symmetry axis with respect to the surface through an angle ϕ defined such that $\phi = 90°$ for the vertical alignment, ca. 0° for the flat alignment in hB1, and ca. 180° for the flat alignment fB1. The dependence of the interaction energy on the two key intermolecular variables, ϕ and the nitrogen to bound-gold bend length R, is depicted in Figure 2 which show scans of the radial potential for various values of ϕ. In producing these curves, values for all other geometrical variables were obtained by linear interpolation using curvilinear internal coordinates between structures N−t1 and hB1, the energies of which are marked on the figure. Note, however, that the intracellular part of the two reference structures were found to be nearly C_{2h} in symmetry, and constraining the coordinates to this point group was found to produce a tiny lowering of the energy. This was found despite possible symmetry lowering associated with the intercellular interactions. As a result, the surfaces shown in Figure 2 were actually obtained with unit cells constrained to C_{2h}.

To aid in the analysis of Figure 2, the optimal bond length and interaction energy for structures constrained to a particular angle ϕ are shown in Figure 3. For vertical alignment, pyridine approaches close to the surface with an equilibrium bond length of 2.46 Å and the bonding is quite strong, 7.3 kcal mol^{-1}. After tilting to $\phi = 60°$ the energy rises 1.5 kcal mol^{-1}, plateauing at around 30° at an energy typical of those of the flat conformations. The bond length increases linearly for angles of less than 45° toward that of the flat structure, 3.4 Å. A rather interesting feature evident from Figure 2 is that the potential becomes quite independent of ϕ in the large-R region around 3.5 Å, indicating minimal resistance to tumbling motion. As a result, the angular forces become very small, small enough to satisfy the geometry optimizer that structure hB1 is a local minimum on the potential-energy surface. In fact, careful examination indicates that this structure is not a local minimum but rather the energy decreases mononotically toward a true local minimum at the vertical structure, N−t1. Given this, it is uncertain as to whether any of the flat structures described in Table 1 and Figure 1 are true local minima. The structures are quite informative, however, in that they indicate that at separations and energies typical of flat structures, there is also minimal resistance to translational motions parallel to the surface.

C. Varying the Coverage for the Flat Configurations. The effect of varying the coverage on the binding energies of the

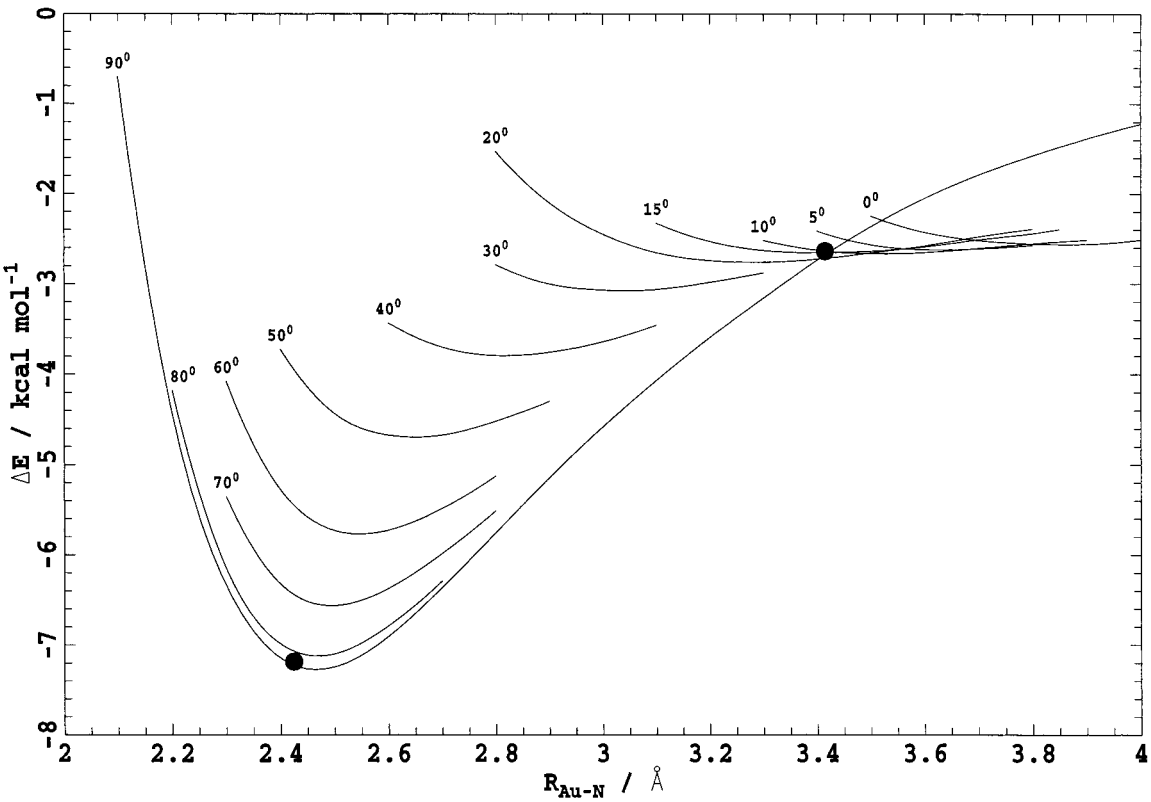

Figure 2. Interaction energy ΔE of adsorbed pyridine on Au(111) as a function of the gold−nitrogen separation R for various values of the angle ϕ between the symmetry axis of the pyridine and the surface. All other curvilinear geometrical variables are linearly interpolated (extrapolated) between their values for the (nearly fully) optimized structures indicated by the solid circles.

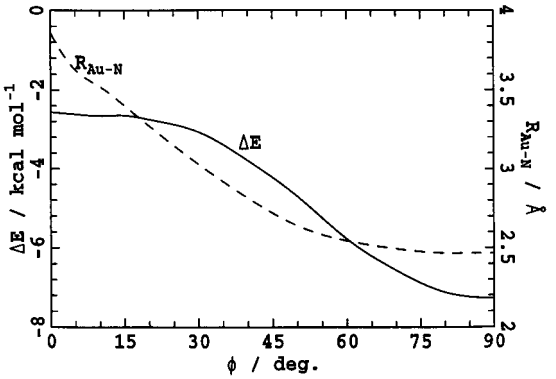

Figure 3. Optimum bond length R and optimal interaction energy ΔE for pyridine on Au(111) constrained such that the angle of the symmetry axis of pyridine with the surface is ϕ; see Figure 2.

flat configurations is difficult to evaluate directly as the adsorbate covers a significant fraction of the area of the (3×3) cell, making size reduction difficult, while larger cells are impractical. However, as the results shown in Table 1 for the (3×3) cell indicate that the attractive energy with the gold surface is insensitive to translation, it appears that the energy variation with coverage should be due primarily to inter-pyridine interactions. Hence, we proceed considering only the interaction between pyridine molecules in different unit cells without inclusion of the underlying gold substrate. At the optimized structure hB1, the inter-pyridine interactions contribute 0.8 kcal mol^{-1} to the binding energy, ca. 40% of the net value. The calculated binding energy of the flat structures, extrapolated to zero coverage, is thus 1.5 kcal mol^{-1}, a rather small value.

It is also possible to extrapolate our results to very high coverage, assuming again that interactions with the surface do not modify the structure of a pyridine monolayer. Due to the boundary conditions used, for all flat structures shown in Figure 1, the pyridines in a given layer are all images of each other and hence the arrangement is ferroelectric. We have optimized the structure of a single pyridine in a monoclinic unit cell with the pyridine parallel to the inclined plane (i.e., $\phi = 0°$), obtaining a net attractive energy of 2.4 kcal mol^{-1} and a unit cell whose inclined-plane surface indicates a packing density of 0.19 ML. This is quite close to the observed[12] packing density of a flat monolayer from electrochemical adsorption at metal−solution interface of 0.22 ML. In addition, we have optimized the structure of two pyridines arranged antiferroelectrically in a unit cell, obtaining the same packing density but with an attractive energy of just 0.5 kcal mol^{-1}. These results suggest that a ferroelectric structure is likely for a flat monolayer, with the experimentally observed slightly higher packing densities perhaps arising from slight puckering of the molecules out of a perfectly planar layer.

D. Varying the Coverage for the Atop Configurations. The atop vertical adsorption of pyridine in structure N−t1 has also been considered at 1/4 ML coverage, considering only an azimuthal orientation in which neighboring pyridine molecules did not intersect. The calculated binding energy is found to be 4.5 kcal mol^{-1}, much less than the 1/9 ML result of 7.3 kcal mol^{-1}. As the interaction energy is expected[20] to decreases with the third power of the length of the unit cell, these results can be extrapolated to yield an adsorption energy at zero coverage of 8.4 kcal mol^{-1}. A similar result is also obtained by considering explicitly the expansion of a similar unit cell containing only the pyridine molecules, after renormalization of the dipole moment and hence the extrapolation method appears sound. There are, however, indications that chemical interactions between the adsorbate and surface are modified at

high coverage. The Au−N bond length is found to increase from 2.43 Å at 1/9 ML to 2.51 Å at 1/4 ML coverage. Also, while no appreciable change in the surface structure is found at 1/9 ML coverage, a buckling of the attached gold atom of 0.1 Å outward is predicted at 1/4 ML. A similar effect has also been found for ammonia bonded to gold(111).[20]

From aqueous solution, monolayers of pyridine on gold are known[12] to tilt somewhat from vertical at the rather high packing density of 0.30 ML. Clearly, the attractive forces between pyridine molecules and between pyridine and solvent molecules overcome the dipole repulsive forces evidenced by our density-functional calculations. The issues involved are considered in detail in section V.

E. Electronic Structure of the Atop Configuration. Adsorption-induced redistributions in the electronic structure of the substrate are reflected through modulation of the work function. These originate from surface dipoles as well as charge transfer between adsorbate and substrate. The work function is computed as the difference between the electrostatic potential in the middle of the vacuum region and the Fermi energy. For a clean gold substrate this was previously calculated to be 5.23 eV.[20] For pyridine absorption, our calculations predict a decrease in the work function of 1.85 and 3.05 eV for the pyridine coverages of 1/9 and 1/4 ML, respectively. Using the Helmholtz equation,[31] which gives a linear relationship between the change in the work function and the adsorbate-induced dipole on the surface, an effective dipole moment of 3.35 D per molecule is obtained for the low-coverage case. This presents an enhancement by 50% from the value of 2.25 D predicted for free pyridine.

To obtain insight into the electronic factors that control the change in the work function and adsorption in general, projected densities of states (PDOS) have been calculated by projecting the wave function onto atom-centered spherical harmonic basis functions, considering only the electron density found within nonoverlapping spheres centered on each atom. The PDOS are displayed in Figure 4. The top and middle panels show the projected densities on the s and p orbitals of the N atom for a free pyridine molecule and for the atop adsorbed molecule (vertically oriented and coordinated via the N atom), respectively. The only significant difference is manifested in the shape and position of the highest occupied molecular orbital (HOMO) $11a_1$, which represents the lone pair, composed of the p_z orbital with some hybridization with the s orbital. Instead of the well-defined prominent peak, characteristic for a free molecule, a broad peak is observed on adsorption, shifted by ∼2 eV below the energy of the noninteracting orbital. In addition to this peak, another small peak appears at an energy of ∼1 eV above that of the unperturbed orbital. The lower panel of the Figure 4 represents the effects of the bonding on the gold surface atom to which the molecule is coordinated. Only the d_{z^2} orbital of the atom is shown, before and after the adsorption, as other orbitals do not undergo large changes. The two peaks in the unperturbed density at ∼2 and ∼4 eV below the Fermi level shift up and down by ∼1 and ∼0.5 eV upon the adsorption. The new peak energies correspond to those of the N p_z orbital in the middle panel. The interaction between the Au d_{z^2} and N p_z is further corroborated by two additional low-lying peaks of a small amplituded in the density of the gold orbital, at the energies that match those of the molecular $8a_1$ and $10a_1$ orbitals. A strong interaction between adsorbate and substrate is apparent but this does not give rise to covalent bonding as the interacting orbitals are all fully occupied. In fact, this interaction can only give rise to weak, orientationally dependent, dispersive bonding.

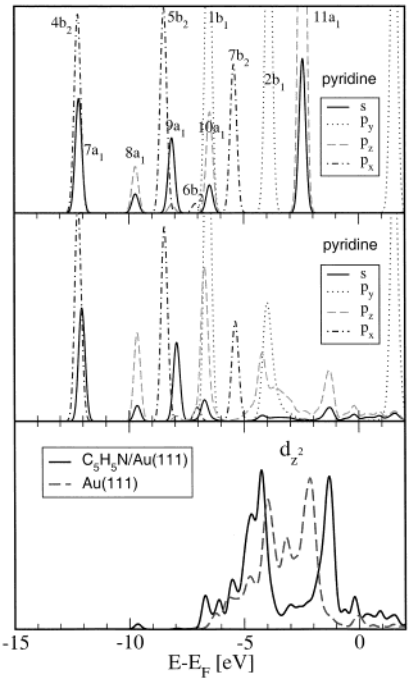

Figure 4. Projected densities of states (PDOS) as a function of the difference between the Kohn−Sham orbital energy E and the Fermi energy E_F on the orbitals of the N atom and its coordinating surface Au atom. Top panel: PDOS on the N atom of a free pyridine molecule, with the energy scale shifted for optimal alignment with the energy scale of the coordinated molecule. Middle panel: PDOS on the N atom of adsorbed pyridine in the vertical orientation. Lower panel: PDOS of the d_{z^2} orbital of the Au atom on the clean and pyridine covered surface, respectively.

Covalent interactions are possible only between the N p_z orbital and the partially filled s orbital of the bonded gold atom, but no such interaction is apparent in the PDOS.

It is possible to consider charge transfer and polarization effects by examining the differential charge density, i.e., the charge density of the whole system from which the densities of the adsorbate and the substrate have been subtracted. The latter are evaluated at the distorted atom geometries taken from the calculation of the adsorbate−substrate complex, rather than for relaxed geometries, to visualize charge flow as arising from the adsorption. Two typical isosurfaces of the differential charge, illustrating the deficit and surplus of electrons, are displayed in Figure 5. Two conclusions can be drawn. First, the adsorption induced density change is rather small, as all isosurfaces that extend over a considerable region of space have very low values. Second, isosurfaces of both negative and positive charge are mainly confined to the lower part of the molecule and the coordinating gold atom. This indicates that the gold(111) to pyridine interaction is locally confined to the gold atom that is directly bonded to the pyridine. Overall, the differential charge density depicts little net charge transfer between adsorbate and substrate, no evidence for charge buildup in the center of the bonding region (another signature of strong covalent bonding), and evidence only of charge redistributions on the bonded atoms reminiscent of charge polarization.

The ability of a computational scheme to correctly represent the charge transfer between two interacting systems is related to its ability to calculate the energy gaps between the orbitals. While ionization energies evaluated for gold and for pyridine are in good agreement with experiment, due to the effect described in section IIIa the orbital energy differences may not be properly depicted. Experimentally, the ionization energies

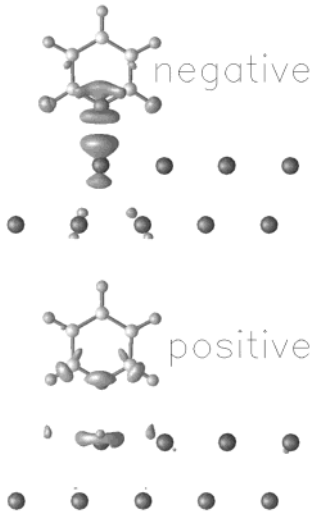

Figure 5. Isosurfaces of differential charge of Au(111)−NH_3(3 × 3). Upper panel: negative value indicating electron deficit (an isovalue of 0.015 e/Å^3) Lower panel: positive value indicating electron surplus (an isovalue of 0.011 e/Å^3).

of pyridine[29] and gold(111)[32] are 9.60 and 5.1 eV, respectively, a gap of 4.5 eV, whereas the calculated energy of the pyridyl lone-pair orbital with respect to the Fermi energy is just 2.5 eV from Figure 4. As a result, our computational method is expected to overestimate charge-transfer contributions and hence our conclusion that such terms are unimportant is reinforced.

IV. Nature of the Bonding

It is interesting to compare the polarization effects indicated by Figure 5 with the effective surface dipole evaluated from the Helmholtz equation. The polarization can be estimated from values of the electric field emitted from the pyridine and the surface and the polarizabilities of pyridine and the attached gold atom. The calculated electric field of a free pyridine molecule (in its adsorbed configuration) at the position of the bound gold atom is 0.0137 au, while that emanating from the surface at the separation of the center of the ring is −0.000 085 au. Using PW91, the calculated[20] polarizability of a gold atom is 37 au. For pyridine, we evaluate the PW91 polarizability using GAUSSIAN-98[33] with the aug-cc-pVDZ basis.[34] The axial component, of relevance hereto, is calculated to be 74 au, while the calculated isotropic value is 63 au, close to the observed value of 64 au.[27] From these data the estimated induced dipole on pyridine is −0.016 D while that at the coordinated Au atom is 1.29 D; adding these to the calculated dipole imoment of the pyridine monomer of 2.25 D predicts a total surface dipole of 3.52 D. The number is in good agreement with the value of 3.35 D deduced using the Helmholtz equation. While this calculation neglects the strong field gradient experienced by the adsorbate (and other effects[20]), the calculated induced moments are qualitatively reflected in the charge distributions shown in Figure 5: the charge shift from nitrogen and two hydrogens upward tends to reduce the pyridine dipole, while the downward shift on the gold atom would result in a dipole moment with the same orientation as that of the molecule. Most significantly, this analysis indicates that charge-transfer contributions are not required in order to understand the calculated changes in the work function due to pyridine adsorption. A charge transfer of just 0.1 e from nitrogen to its attached gold atom would be sufficient to account for the 1.2 D change in effective dipole moment, and so net adsorbate to metal charge transfer is apparent.

From the above field strengths and induced dipole moments, the contribution of the polarization to the adsorption energy can also be estimated. It amounts to 2.1 kcal mol^{-1} and arises almost entirely from the polarization of the gold. This energy is well below the estimated zero-coverage adsorption energy of 7.3 kcal mol^{-1}. Since we have argued that covalent and charge-transfer effects are minimal, the remaining source of the binding energy must be dispersion. The dispersive energy may be estimated using the well-known London expression:[35]

$$V_{\mathrm{disp}} = -\frac{3}{2}\frac{I(\mathrm{C_5H_5N})I(\mathrm{Au})}{I(\mathrm{C_5H_5N}) + I(\mathrm{Au})}\frac{\alpha(\mathrm{C_5H_5N})\alpha(\mathrm{Au})}{R^6} \qquad (1)$$

where R is the separation between the Au and ring center, I are ionization energies,[27] and α are isotropic polarizabilities.[27] This term contributes a binding energy to the atop configuration of 3.3 kcal mol^{-1}, again much less than the PW91-calculated binding. It, however, uses the gold to pyridine-ring center distance of 3.8 Å and ignores the previously identified strong short-range dispersive interaction between the N p_z orbital and the d_{z^2} orbital on the bound gold atom. Our analysis suggests that, in reality, dispersive interactions are likely to provide important contributions to the binding in this system.

In general, modern density functionals provide poor descriptions of dispersive interactions, at best treating them empirically via modified covalent terms. We have shown that PW91 is typical of other functionals in this regard.[20] Hence the correct physical cause of the binding as perceived by PW91 is difficult to isolate and possibly flawed in nature. On the basis of the proven performance of PW91 in modeling the somewhat analogous binding between ammonia and gold,[18,20] we anticipate that the calculated binding energy for the pyridine atop configuration is qualitatively realistic. Quantitatively, a correction factor of 3 kcal mol^{-1} or ca. 25% has been estimated[18] for the gold−ammonia case, and if this is applied to gold−pyridine, then the calculated binding energy at zero coverage would increase from 8.4 to ca. 11 kcal mol^{-1}.

From eq 1, the anticipated dispersion energy for the flat configurations at R = 3.4 Å is 6.4 kcal mol^{-1}. While this attraction must be balanced by the exchange repulsion terms in order to establish a minimum in the potential-energy surface, the PW91 calculated binding energies of 1.5 kcal mol^{-1} at zero coverage appear to significantly underestimate the interaction. As a result, the calculated energy required in order to flatten a pyridine molecule on the surface of order 5 kcal mol^{-1} evident in Table 1 is likely to be significantly too large.

V. Relation to Solution Studies

There are continuing experimental investigations of the adsorption of pyridine on gold(111) from typically aqueous solution (see, e.g., the review by Lipkowski and Stolberg[12]). The orientation of the molecule, as deduced inter alia from chronocoulometry,[36] surface-enhanced infrared absorption,[37] scanning-tunneling spectroscopies,[37,38] and difference frequency generation,[39] has been shown to depend on the potential of the Au(111) electrode. At potentials well positive to the point of zero charge, pyridine is known to be bound via the N atom in the atop position. As the potential moves through the zero-charge point to negative values, a 2-dimensional phase change occurs with the molecule tending to a nearly flat position on the surface. The orientation is also influenced by the degree of coverage.[40] Basically, our present calculations reflect this scenario, with positive potentials predicted to attract the nitrogen lone pair and negative potentials predicted to repel the molecular dipole. They

adequately predict the packing density of the flat layer but are insufficient in either scope and/or accuracy to explain the high packing density observed for the atop structure.

The electrochemical experiments show that pyridine is more strongly adsorbed at Au(111) than at Ag(111) surfaces. This has been attributed[12] to the molecular a_1, a_2, and b_1 filled orbitals lying closer by ca. 1 eV to the Fermi edge in the former case, resulting in increased coupling through metal s and p bands. On the basis of our calculations, the change in the Fermi energy would also be predicted to be the primary factor, except that modulation of the dispersive interactions with the metal d_{z^2} band would be expected to be the major contributor.

Quantitatively, the electrochemical experiments[12] suggest a value of ca. -10 kcal mol^{-1} for the Gibbs energy of adsorption from aqueous solution to the Au(111) surface. To relate this to a gas-phase binding energy, corrections must be introduced for the solvation of the pyridine and for the changes in the electrode−solvent interface. The hydration enthalpy of pyridine is known[41] to be -12 kcal mol^{-1} and so it appears that the sum of the pyridine−surface interaction energy, intermonolayer pyridine−pyridine interactions, solvation changes, and entropy effects needs to be around -22 kcal mol^{-1}. While the inter-pyridine interactions at the structures dictated by our unit cells are repulsive, the propensity for pyridine to tilt, shown in Figure 3, combined with the known stability of staggered arrangements,[42−44] suggests that overall attractive interactions are likely. An aspect of this may be that the PW91 calculations fail significantly in their treatment of the inter-pyridine attractive dispersion energy. Also, as the exposed hydrogens of the solvent water molecules near the interface would prefer to interact with an exposed aromatic π cloud than with a gold surface, interface effects are also expected to enhance the binding. Nevertheless, these experimental results are suggestive that the corrected zero-coverage PW91 binding of ca. 11 kcal mol^{-1} discussed in the previous section underestimates the magnitude of the interaction.

Another point of quantitative comparison with the electrochemical work is the value of the effective dipole moment of the adsorbed pyridine. In solution, this may be deduced from the shift of potential of zero charge accompanying adsorption in the vertical position and has been estimated[36] to be 0.9 D, in stark contrast to our predicted low-coverage UHV value of 3.35 D. While the calculated value represents a sizable enhancement of the gas-phase dipole moment of pyridine (2.25 D), the solution value represents a sizable reduction. One possible explanation of this discrepancy is that the experimental measurement actually yields μ/ϵ, where ϵ is the effective dielectric constant of the doublel layer; a value of $\epsilon = n^2$ (where n is the effective refractive index) is used in determining μ. In reality, the dielectric constant could be much larger than this. Other possible causes include tilting of the pyridine molecules from vertical, an effect that would reduce the observed normal component of the surface dipole, and encapsulation of solvent water molecules, oriented with their hydrogens toward the surface in order to interact with the aromatic π cloud, whose dipole moments would require inclusion. The experimental value actually involves all changes that take place inside the double layer near the surface and may not reflect simply the adsorbate−surface interaction. Finally, the dependence of the potential of zero charge on the dipole moment may be more complex than has previously been recognized.

VI. Conclusions

The adsorption of pyridine on metallic surfaces such as gold(111) is an important and well-studied process, yet features of the intrinsic binding such as the nature, strength, and flexibility of the binding, and the value of the induced dipole moment, remain poorly defined. We conclude that the binding is dispersive in nature, with significant contributions from charge polarization effects but minimal contributions from charge transfer and covalent bonding. Consequently, quantitative calculations are difficult to apply, as Hartree−Fock theory is inappropriate while density-functional theory is problematic. Nevertheless, our calculations using the PW91 density functional have led to the prediction of a binding energy of 8.4 kcal mol^{-1} after extrapolation to zero coverage. Based on an analogy with gold−ammonia binding, this value may underestimate the real one by 3 kcal mol^{-1}. Even with this correction, the calculated biding may be too small to account for the known free-energy changes of adsorption of pyridine from aqueous solution. A sizable energy of ca. 5 kcal mol^{-1} is predicted for the conversion of the adsorbate from its lowest-energy atom configuration to a structure with the pyridine lying flat on top of the surface; due to the greater importance of dispersive interactions for flat configurations, this difference is likely to be overestimated. It is calculated that the dipole moment of pyridine is enhanced by 1.1 D on atop adsorption, in contrast to a reduction of 0.9 D implied from observed electrochemical data in aqueous solution. We suggest that this discrepancy could be due to a combination of tilting of the pyridine from vertical, and from organization of the first solvent layer about the pyridine molecules. Hence, from both energetic and electrostatic arguments, the properties of pyridyl monolayers on gold appear to be strongly influenced by interactions with the solvent.

One feature of the calculated potential surface that is expected to be robust is that it is very flat for small changes in angle from the vertical structure, indicating that pyridine may tilt to angles of order 30° from vertical with minimal energy cost. The gold−pyridine interaction is thus seen to be both reasonably strong and highly flexible. As a result, pyridine may be an effective "alligator clip" for use in molecular electronic applications, binding molecules securely yet flexibly to gold electrodes. Other linkages in common use such as thiols provide much stronger but far less flexible binding, adding restrictions to ones ability to fabricate electrode−single molecule−electrode assemblies.

Supporting Information Available: Calculated structure and orbital energies for isolated pyridine, with comparisons to observed structural and ionization-energy data. This material is available free of charge via the Internet at http://pubs.acs.org.

Acknowledgment. The work was supported by the Australian Research Council. The use of supercomputer facilities at the Australian Partnership for Advanced Computing (APAC) is gratefully acknowledged. We thank Professor Roger Parsons (University of Southampton) for most helpful comments.

References and Notes

(1) Somorjai, G. A. *Introduction to Surface Chemistry and Catalysis*; Wiley: New York, 1994.

(2) Reed, M. A.; Zhou, C.; Muller, C. J.; Burgin, T. P.; Tour, J. M. *Science* **1997**, *278*, 252.

(3) Chan, J.; Reed, M. A.; Rawlett, A. M.; Tour, J. M. *Science* **1999**, *286*, 1550.

(4) Emberly, E. G.; Kirczenow, G. *Phys. Rev. B* **1998**, *58*, 10911.

(5) Hall, L. E.; Reimers, J. R.; Hush, N. S.; Silverbrook, K. *J. Chem. Phys.* **2000**, *112*, 1510.

(6) Reimers, J. R.; Shapley, W. A.; Lambropoulos, N. A. *Ann. N. Y. Acad. Sci.*, in press.

(7) Seminario, J. M.; De La Cruz, C. E.; Derosa, P. A. *J. Am. Chem. Soc.* **2001**, *123*, 5616.
(8) Crossley, M. J.; Burn, P. L.; Langford, S. J.; Prashar, J. K. *J. Chem. Soc., Chem. Commun.* **1995**, 1921.
(9) Crossley, M. J.; Prashar, J. K. *Tetrahedron Lett.* **1997**, *38*, 6751.
(10) Reimers, J. R.; Hall, L. E.; Crossley, M. J.; Hush, N. S. *J. Phys. Chem. A* **1999**, *103*, 4385.
(11) Hébert, P.; Le Rilie, A.; Zheng, W. Q.; Tadjeddine, A. *J. Electroanal. Chem.* **1998**, *447*, 5.
(12) Lipkowski, J.; Stolberg, L. In *Adsorption of molecules at metal electrodes*; Lipkowski, J., Ross, P. N., Eds.; VCH: New York, 1992; p 171.
(13) Mate, C. M.; Somorjai, G. A.; Tom, H. W. K.; Zhu, X. D.; Shen, Y. R. *J. Chem. Phys.* **1988**, *88*, 441.
(14) Haq, S.; King, D. A. *J. Phys. Chem.* **1996**, *100*, 16957.
(15) Demuth, J. E.; Christmann, K.; Sanda, P. N. *Chem. Phys. Lett.* **1980**, *76*, 201.
(16) Bader, M.; Haase, J.; Frank, K.-H.; Puschmann, A. *Phys. Rev. Lett.* **1986**, *56*, 1921.
(17) Tadjeddine, A.; Flament, J. P. *Chem. Phys.* **2001**, *265*, 27.
(18) Lambropoulos, N. A.; Reimers, J. R.; Hush, N. S. *J. Chem. Phys.* **2002**, *116*, 10277.
(19) Perdew, J. P.; Wang, Y. *Phys. Rev. B* **1992**, *45*, 13244.
(20) Bilić, A.; Reimers, J. R.; Hush, N. S.; Hafner, J. *J. Chem. Phys.* **2002**, *116*, 8981.
(21) Kristyán, S.; Pulay, P. *Chem. Phys. Lett.* **1994**, *229*, *175*.
(22) Kresse, G.; Hafner, J. *Phys. Rev. B* **1993**, *47*, RC558.
(23) Kresse, G.; Furthmüller, J. *Comput. Mater. Sci.* **1996**, *6*, 15.
(24) Vanderbilt, D. *Phys. Rev. B* **1990**, *41*, 7892.
(25) Kresse, G.; Hafner, J. *J. Phys. Condens. Matter* **1994**, *6*, 8245.
(26) Methfessel, A.; Paxton, A. T. *Phys. Rev. B* **1989**, *40*, 3616.
(27) Lide, D. R., Ed. *CRC Handbook of Chemistry and Physics*; CRC Press: Boca Raton, FL, 1996.
(28) Cai, Z.-L.; Reimers, J. R. *J. Phys. Chem. A* **2000**, *104*, 8389.
(29) Kimura, K.; Katsumata, S.; Achiba, Y.; Yamazaki, T.; Iwata, S. *Handbook of He I Photoelectron Spectra of Fundamental Organic Molecules*; Halstead: New York, 1981.
(30) Walker, I. C.; Palmer, M. H.; Hopkiik, A. *Chem. Phys.* **1989**, *141*, 365.
(31) Somorjai, G. A. *Introduction to Surface Chemistry and Catalysis*; Wiley: New York, 1994; p 371.
(32) Jackschath, C.; Rabin, I.; Schulze, W. *Ber. Bunsen-Ges. Phys. Chem.* **1992**, *96*, 1200.
(33) Frisch, M. J.; Trucks, G. W.; Schlegel, H. B.; Scuseria, G. E.; Robb, M. A.; Cheeseman, J. R.; Zakrzewski, V. G.; Montgomery, J. A.; Stratmann, R. E.; Burant, J. C.; Dapprich, S.; Millam, J. M.; Daniels, A. D.; Kudin, K. N.; Strain, M. C.; Farkas, O.; Tomasi, J.; Barone, V.; Cossi, M.; Cammi, R.; Mennuci, B.; Pomelli, C.; Adamo, C.; Clifford, S.; Ochtersi, J.; Patterson, G. A.; Ayala, P. Y.; Cui, Q.; Morokuma, K.; Malick, D. K.; Rabuck, A. D.; Raghavachari, K.; Foresman, J. B.; Cioslowski, J.; Ortiz, J. V.; Stefanov, B. B.; Liu, G.; Liashenko, A.; Piskorz, P.; Komaromi, I.; Gomperts, R.; Martin, R. L.; Fox, D. J.; Keith, T.; Al-Laham, M. A.; Peng, C. Y.; Nanayakkara, A.; Gonzalez, G.; Challacombe, M.; Gill, P. M. W.; Johnson, B. G.; Wong, W. Chen.; Wong, M. W.; Andres, J. L.; Head-Gordon, M.; Replogle, E. S.; Pople, J. A. *Gaussian 98*, revision A7; Gaussian Inc.: Pittsburgh, PA, 1998.
(34) Dunning, T. H., Jr.; Harrison, R. J. *J. Chem. Phys.* **1992**, *96*, 6796.
(35) Alberty, R. A.; Silbey, R. J. *Physical Chemistry*, 2nd ed.; Wiley: New York, 1997.
(36) Stolberg, L.; Morin, S.; Lipkowski, J.; Irish, D. E. *J. Electroan. Chem.* **1991**, *307*, 241.
(37) Cai, W.-B.; Wan, L.-J.; Noda, H.; Hibino, Y.; Ataka, K.; Osawa, M. *Langmuir* **1998**, *14*, 6992.
(38) Andressen, G.; Vela, M. E.; Salvarezza, R. C.; Arvia, A. J. *Langmuir* **1997**, *13*, 6814.
(39) Tadjeddine, A.; Le Rille, A.; Pluchery, O.; Hebert, P.; Zheng, W. Q.; Marin, T. *Nucl. Instrum. Methods Phys. Res.* **1999**, *A429*, 481.
(40) Gomez, M. M.; Vara, J. M.; Hernandez, J. C.; Salvarezza, R.; Arvia, A. J. *J. Electroan. Chem.* **1999**, *474*, 7481.
(41) Spencer, N. N.; Holmboe, E. S.; Kirshenbaum, M. R.; Barton, S. W.; Smith, K. A.; Wolbach, W. S.; Powell, J. F.; Chorazy, C. *Can. J. Chem.* **1982**, *60*, 1184.
(42) Cunha, F.; Tao, N. J.; Wang, X. W.; Jin, Q.; Duong, B.; D'Agnese, J. *Langmuir* **1996**, *12*, 6410.
(43) Pinheiro, L. S.; Temperini, M. L. A. *Surf. Sci.* **1999**, *441*, 53.
(44) Hunter, C. A.; Sanders, J. K. M. *J. Am. Chem. Soc.* **1990**, *112*, 5525.